Benchmark calculations on residue production within the EURISOL DS project; Part I: thin targets

J.C. David, V. Blideanu, A. Boudard, D. Doré, S. Leray, B. Rapp, D. Ridikas, N. Thiollière
CEA Saclay, DSM/DAPNIA, 91191 Gif-sur-Yvette, France
E-mail : jean-christophe.david@cea.fr

1. Introduction

The European Community decided to support the design study and R&D for a next generation ISOL RIB facility able to increase by a few orders of magnitude the exotic beam intensity and availability in Europe in this initiative, named EURISOL DS project (European Isotope Separation On Line Design Study) [1].

Although some valuable experience is already available from presently operating ISOL facilities world wide, the design of a new generation RIB factory requires specific and validated modelling tools. In this context, detailed simulations should be performed in order to optimise the RIB production in terms of target geometry and materials, incident particle types and their energy, etc. Equally, the radioprotection and safety issues should be addressed and will be based on detailed calculations of particles fluxes, induced radioactivity and resulting dose rates. Benchmark calculations on particle production have already been done by B. Rapp *et al.* [2]. Concerning residue production M. Felcini and A. Ferrari performed a benchmark using the FLUKA code at proton energies around 1 GeV [3]. This paper deals with similar calculations and comparison with experimental data on residue production but with the MCNPX2.5.0 transport code [4], where several spallation models are available.

The previous EURISOL-RTD project [5] proposed to use a primary proton beam with energy around 1 GeV. Two types of production targets could be used: a) direct target, where the radioactive nuclei are produced in the target interacting directly by the primary proton beam including the secondary particles (mainly neutrons but also light charged particles), and b) two-stage fission-target, where the nuclei are produced by secondary neutrons provided from spallation reactions in a target-converter surrounding the secondary target. The production target or target-converter materials suggested by the tasks T2 (*multi-MW target station*), T3 (*direct target*) and T4 (*fission target*) are U, Pb, Hg, W, Ta and Be as defined by the baseline parameters [6].

To validate the codes one had to find the data which were obtained with the projectiles, energy beams and target materials discussed above, and then decide which physics models should be benchmarked. In MCNPX2.5.0 we can use 10 spallation models (or to be more precise, model combinations, namely Intra-Nuclear Cascade model ⊕ Deexcitation model). Thanks to the previous studies (HINDAS [7] and references therein) and the results obtained on some mass distributions of reaction products, one was able to select some of them rapidly, what allowed to limit the number of calculations to be performed.

We have begun this benchmark study using mass distribution data of reaction products obtained at GSI [8] in inverse kinematics. This step allowed us a first selection among the 10 models; in this way the first insight of the quality of the models was obtained. Then, in a second part, experimental mass distributions for some elements, which either are interesting as RIBs or important due to the safety and radioprotection issues (e.g. α or high energy γ emitters), will be also compared to model calculations. These data [8] have been obtained for an equivalent 0.8 or 1.0 GeV proton beam, which is approximately the proposed projectile energy. We note that in realistic thick targets the proton beam will be slowed down and some secondary particles are produced. Therefore, the residual nuclei production at lower energies is also important. For this reason, we also performed in the third part of this work some excitation function calculations and the associated data obtained with γ-spectroscopy [9], [10] to test the models in a wide projectile energy range.

2. Mass distributions

Residue production data obtained at FRS [8] (GSI) during last years have been intensively used to test and improve spallation models (e.g., HINDAS project [7]). Inverse kinematics measurement technique was used to obtain this data, namely the target was made of hydrogen and the projectiles were beams of uranium, lead, gold or iron with energies around 1 A·GeV In the present work the goal is to recommend the best available model(s) within MCNPX2.5.0 for the spallation reaction studies including neutron production for EURISOL-DS.

Fig. 1 shows all 10 model combinations in MCNPX2.5.0 for the reaction ^{238}U(1A.GeV) + p together with corresponding data for the mass distribution of reaction products. Similar quality results are obtained also for ^{208}Pb, ^{197}Au and ^{56}Fe on hydrogen target.

Clearly the Dresner/ORNL evaporation/fission model cannot be used to describe this observable. Combined to RAL, Dresner model gives quite reasonable results, except with the Bertini intranuclear cascade model. On the other hand, some calculations performed with lead show significant discrepancies in the fission part as shown in Fig. 2. The Abla evaporation/fission model gives rather good results in combination with INCL4 and Isabel, whereas with Bertini the nucleus production via evaporation is overestimated. CEM2k shows the same difficulty to reproduce the evaporation part (see Fig. 1).
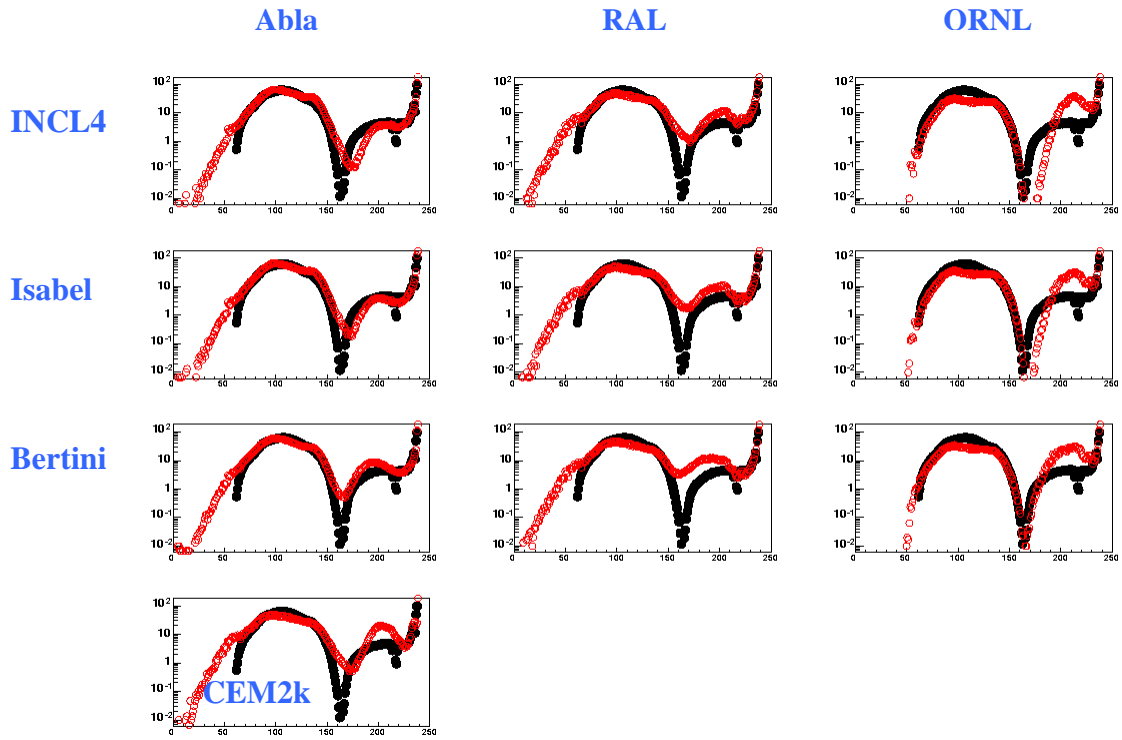
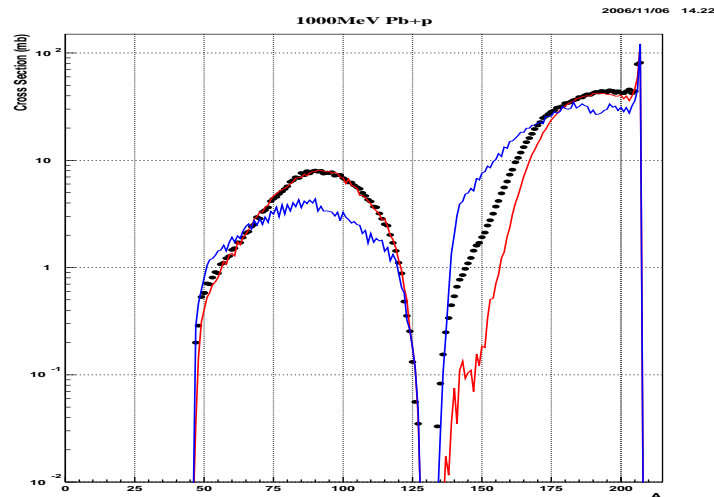**Figure 1:** *Mass distribution of the reaction products from* $^{238}U(1A.GeV)+p$. *GSI Data [8] are in black and model calculations are in red for the ten model combinations available in MCNPX2.5.0. Intra-Nuclear Cascades used are INCL4 [11], Isabel [12] and Bertini [13] (the three first lines), and combined to various evaporation/fission models, which are Abla [14], Dresner [15]/RAL[16] and Dresner/ORNL[17] (the three columns). The last graph (bottom left) is the stand alone package CEM2k [18]. Cross sections are given in mb.*

Figure 2: *Mass distributions for the reaction products from* $^{208}Pb(1A.GeV)+p$. *GSI Data [8] are in black and model calculations are in red for INCL4/Abla and blue for Bertini/Dresner/RAL.*

Using the results presented in Figs. 1 and 2 we decided to limit our study not only to the INCL4/Abla and Isabel/Abla model combinations (they give the best agreement with data) but also to keep CEM2k, which is still being improved (a new version of this model, called CEM03 [19], recently became available for the beta users of MCNPX, but not yet via RSICC distribution services [20]). We have to note that new versions of INCL4 and Abla are also planned and should be available in a next release of MCNPX.

With Fig. 3 we try to quantify our confidence level for the three chosen models on the four nuclei measured at FRS (GSI): uranium (a), lead (b), gold (c), and iron (d). The ratios, calculation/data, for all mass distributions are within a factor 2 for the fission part, except for the very light and heavy fission products, which are produced with low yields. The factor 2 is also true for the other residues, except the ones obtained after a long evaporation phase.
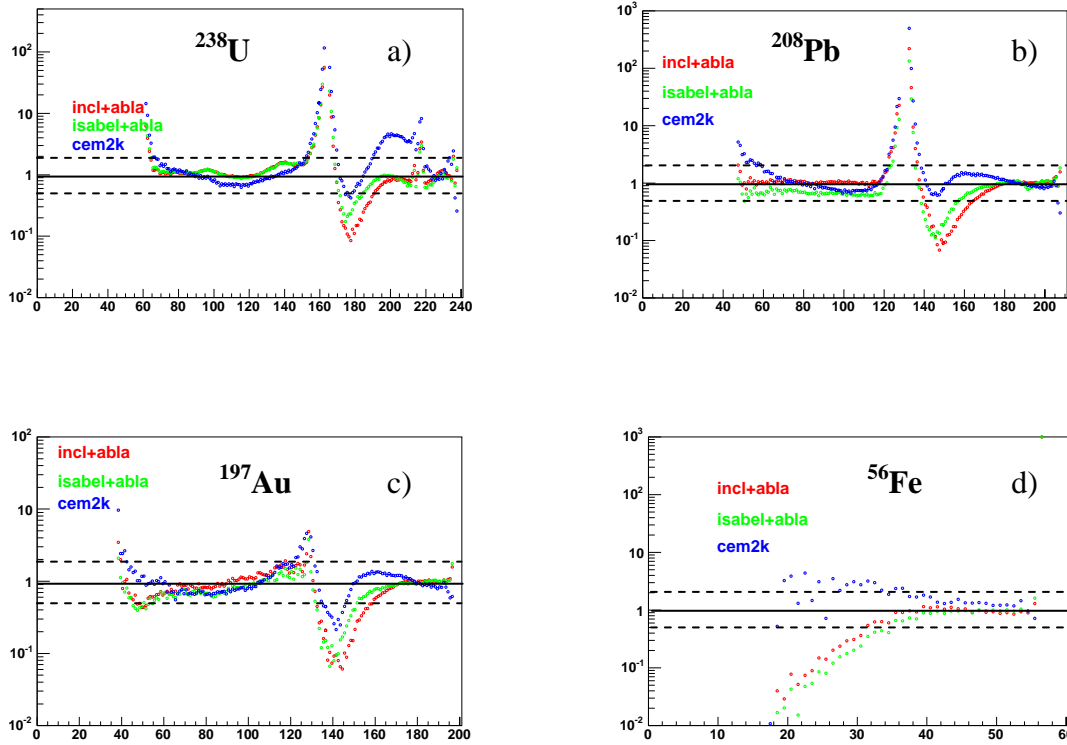

Figure 3: *Calculation/Data ratios for mass distributions for the reactions $^{238}U(1A.GeV)+p$ (a), $^{208}Pb(1A.GeV)+p$ (b), $^{197}Au(0.8A.GeV)+p$ (c) and $^{56}Fe(1A.GeV)+p$ (d) . GSI Data [8] are used and models showed are INCL4/Abla in red, Isabel/Abla in green and CEM2k in blue.*

3. Isotopic distributions

Figs. 4 to 7 represent isotopic distributions for the same four nuclei (U, Pb, Au, Fe). Due to a very huge number of elements, here we selected only those which can play an important role in the radioprotection. Table 1, taken from the paper of M. Felcini and A. Ferrari [3], lists these isotopes.

INCL4 and Isabel have a rather similar behaviour compared to CEM2k. The factor 2 observed for the mass distributions remains valid for INCL4/Abla and Isabel/Abla for the fission part, but for isotopes closer to the initial nucleus, the calculation/data ratios can sometimes be bigger than 2 (e.g., see ^{238}U for Z=92 or 90 in Fig. 4a.). As mentioned

4

previously, isotopes obtained by a long evaporation stage are badly reproduced (e.g., Z=64, worse for ^{208}Pb (Fig. 5) than for ^{197}Au (Fig. 6)), whereas good for ^{238}U (Fig. 4a), since it is then a fission and not an evaporation product.
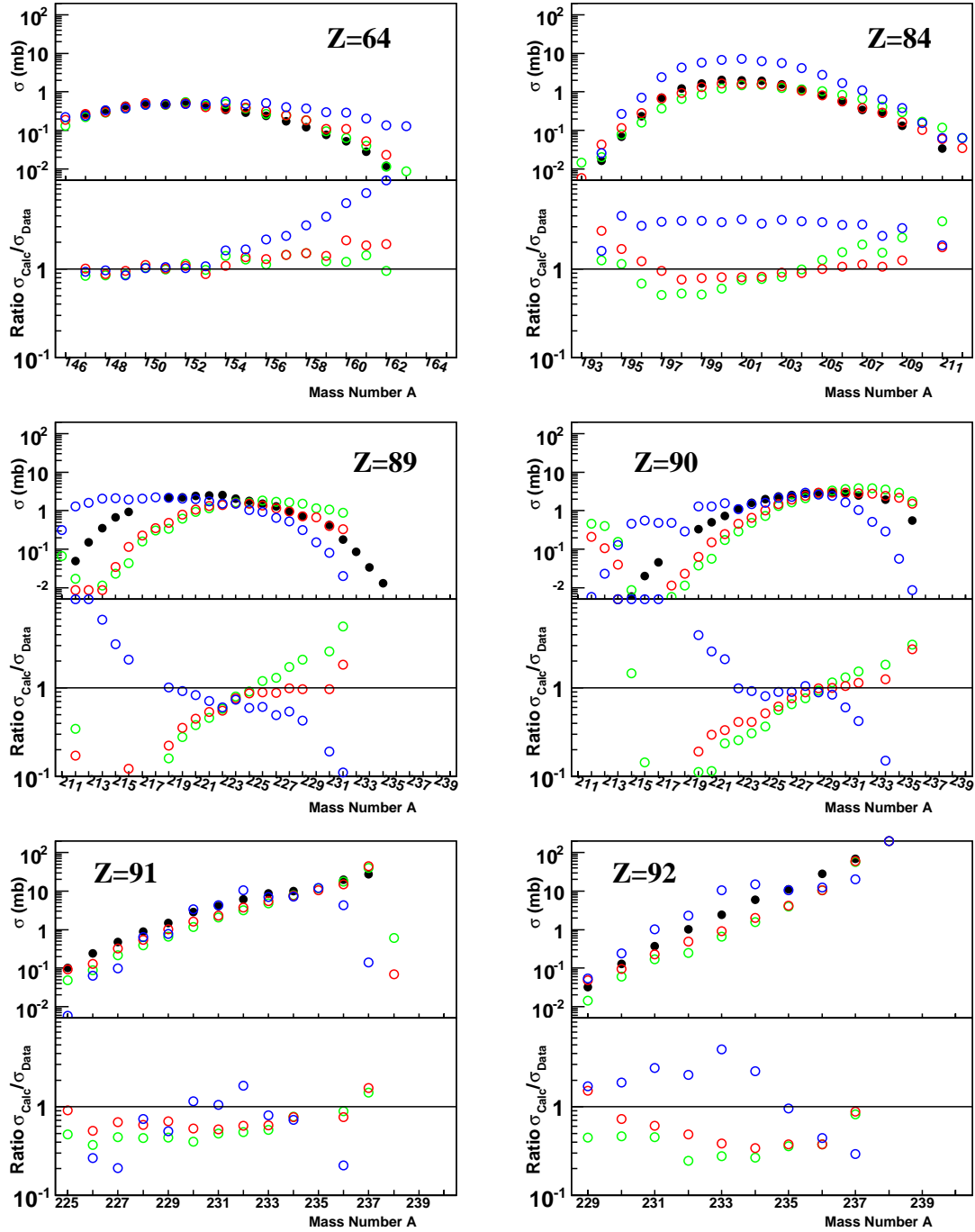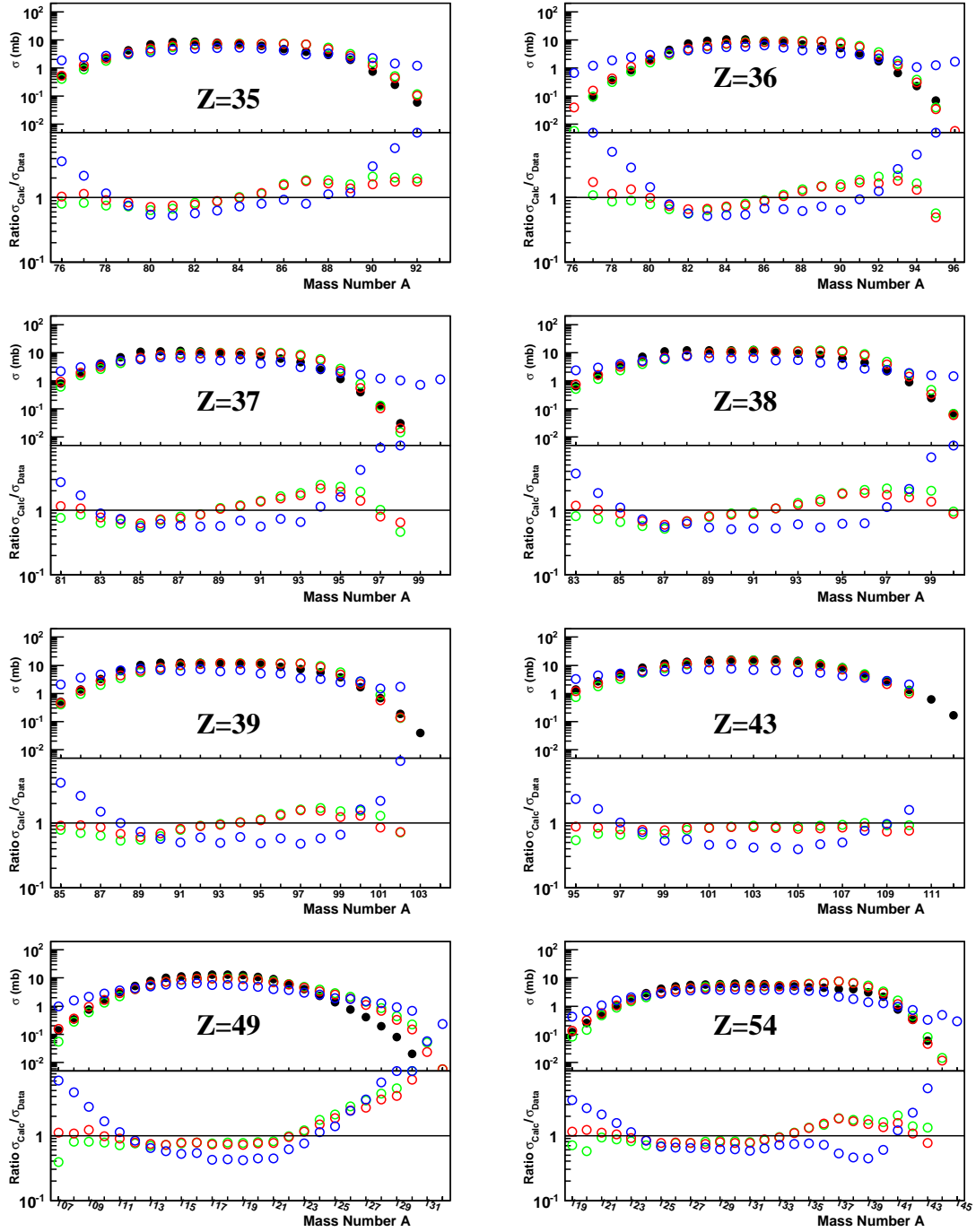

Figure 4a: *Isotopic reaction product distributions from ^{238}U(1A.GeV)+p. For each element absolute cross sections (upper part) and calculation/data ratios (lower part) are plotted. GSI Data [8] in black are used and models shown are INCL4/Abla in red, Isabel/Abla in green and CEM2k in blue.*
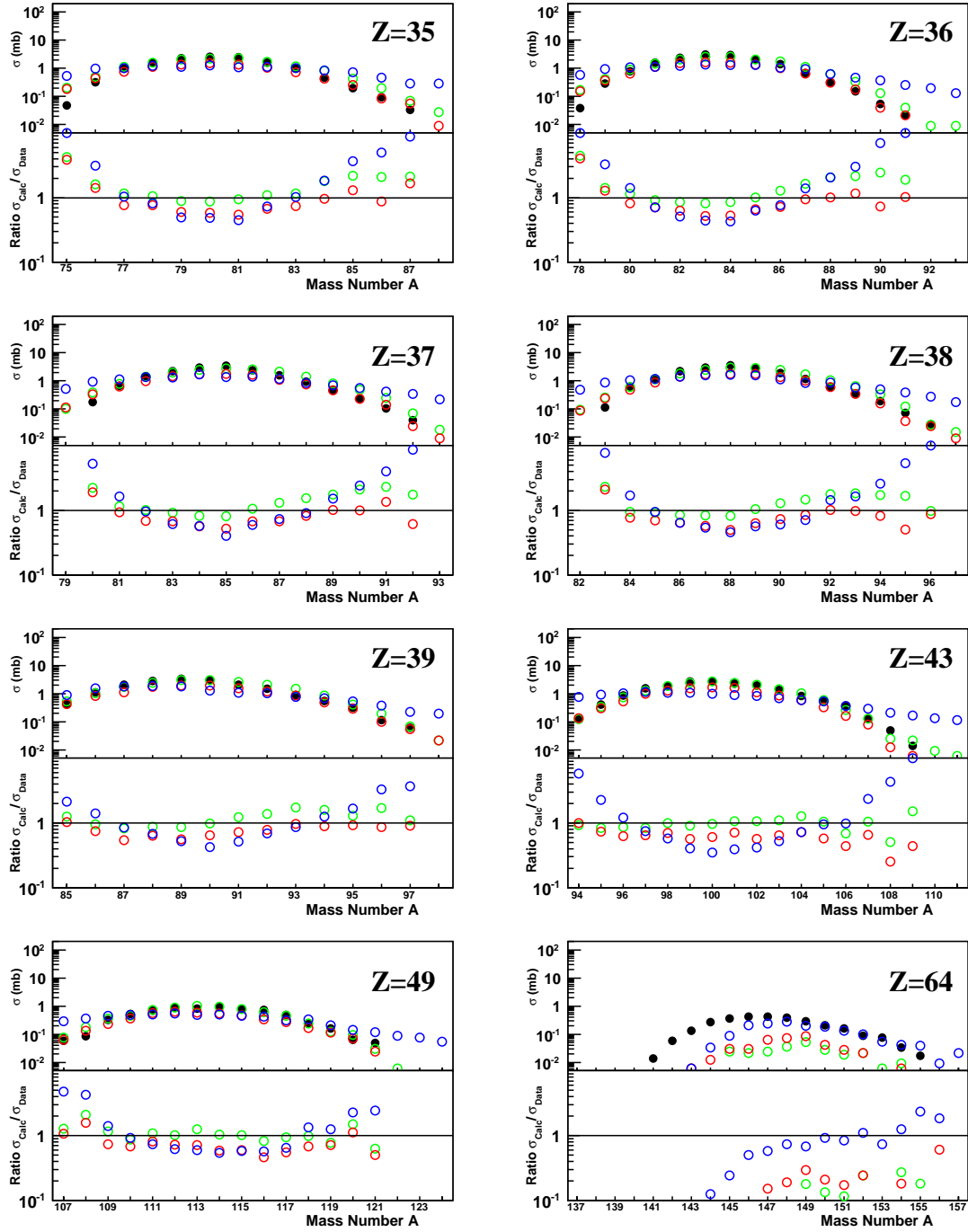
Figure 4b: *Isotopic reaction product distributions from $^{238}U(1A.GeV)+p$. For each element absolute cross sections (upper part) and calculation/data ratios (lower part) are plotted. GSI Data [8] in black are used and models shown are INCL4/Abla in red, Isabel/Abla in green and CEM2k in blue.*
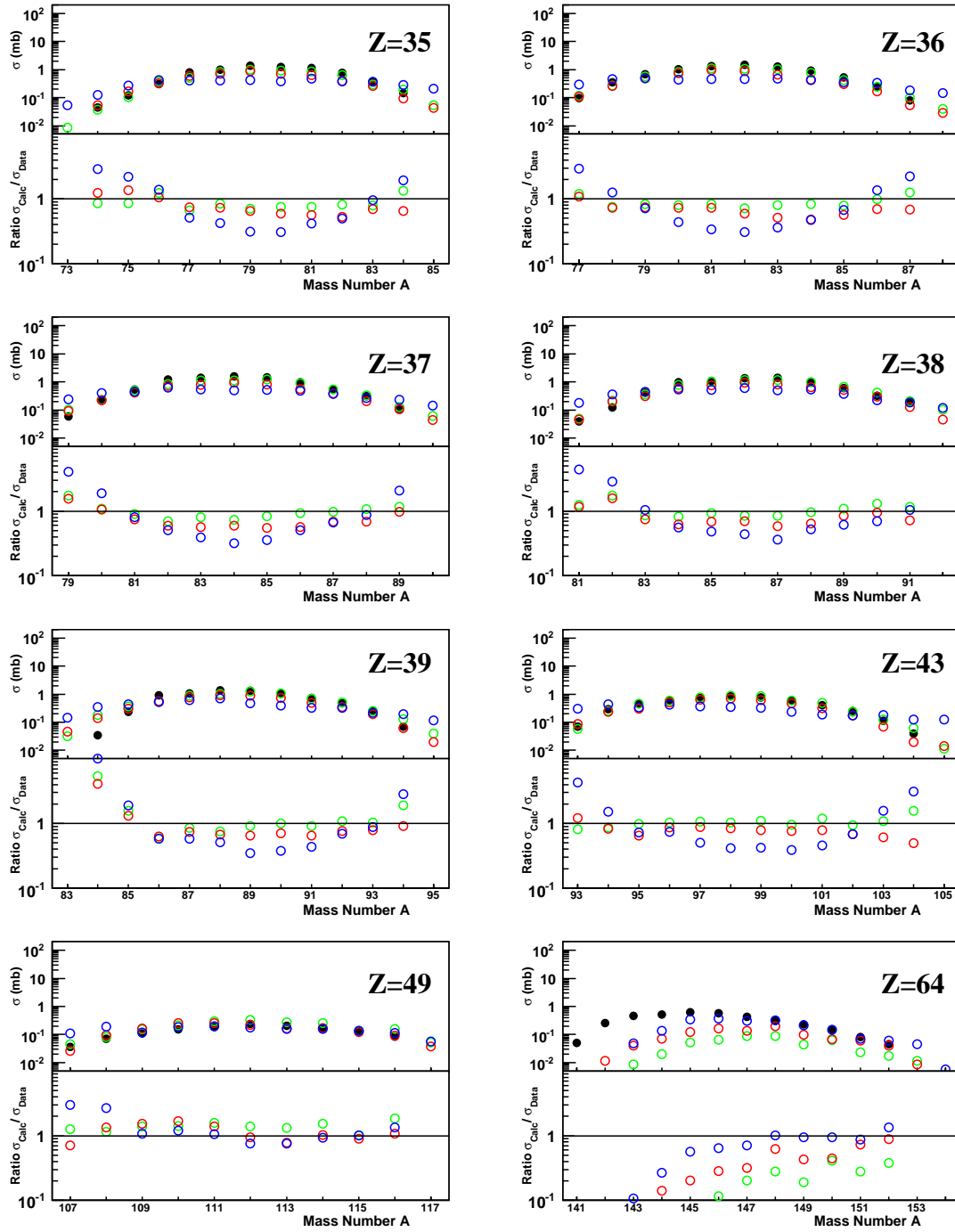
Figure 5: *Isotopic reaction product distributions from $^{208}Pb(1A.GeV)+p$. For each element absolute cross sections (upper part) and calculation/data ratios (lower part) are plotted. GSI Data [8] in black are used and models shown are INCL4/Abla in red, Isabel/Abla in green and CEM2k in blue.*

Figure 6: *Isotopic reaction product distributions from $^{197}Au(0.8A.GeV)+p$. For each element absolute cross sections (upper part) and calculation/data ratios (lower part) are plotted. GSI Data [8] in black are used and models shown are INCL4/Abla in red, Isabel/Abla in green and CEM2k in blue.*
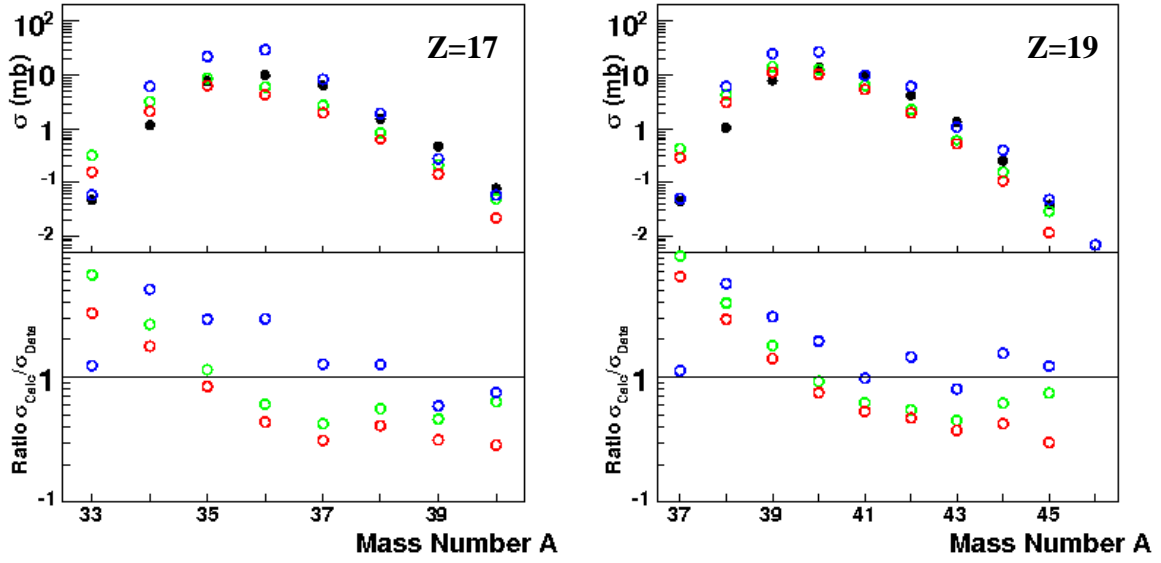
Figure 7: *Isotopic reaction product distributions from $^{56}Fe(1A.GeV)+p$. For each element absolute cross sections (upper part) and calculation/data ratios (lower part) are plotted. GSI Data [8] in black are used and models shown are INCL4/Abla in red, Isabel/Abla in green and CEM2k in blue.*

α emitter isotopes				β/γ emitter isotopes			
Nuclide	Symbol	Z	A	Nuclide	Symbol	Z	A
Gadolinium	Gd	64	148	Chlorine	Cl	17	38
Polonium	Po	84	208,209	Potassium	K	19	44
Actinium	Ac	89	227	Gallium	Ga	31	66
Thorium	Th	90	228,229,230,232	Bromine	Br	35	74
Protactin.	Pa	91	231	Krypton	Kr	36	89
Uranium	U	92	232,238	Rubidium	Rb	37	80,88
				Strontium	Sr	38	80
				Yttrium	Y	39	94,95
				Technet.	Tc	43	104
				Indium	In	49	120
				Xenon	Xe	54	137

Table 1: *A list of major radioactive isotopes being emitters of α, β and γ radiation as from Ref. [3].*

4. Excitation functions

Sources of RIBs are produced with a thick spallation target impinged by high energy protons. These primary protons are slowed down in the target and then spallation reactions take place over a wide projectile energy range. Moreover, secondary emitted particles can also induce spallation reactions. For these reasons models have to be tested not only with the energy of the primary beam, what has been done previously, but also with lower energies. Excitation functions, i.e. isotope production cross sections for several projectile energies, are the observables to be used for this purpose.

Fig. 8 shows some fission products obtained with a lead target and protons from ~70 MeV up to 2.6 GeV [9]. Models plotted are INCL4/Abla and Bertini/Dresner/RAL. We plotted only these two models because the time needed to run a model for all energies can be around one week and even more, and Bertini is the fastest one. Once again INCL4/Abla gives good results, especially compared to Bertini/Dresner/RAL.
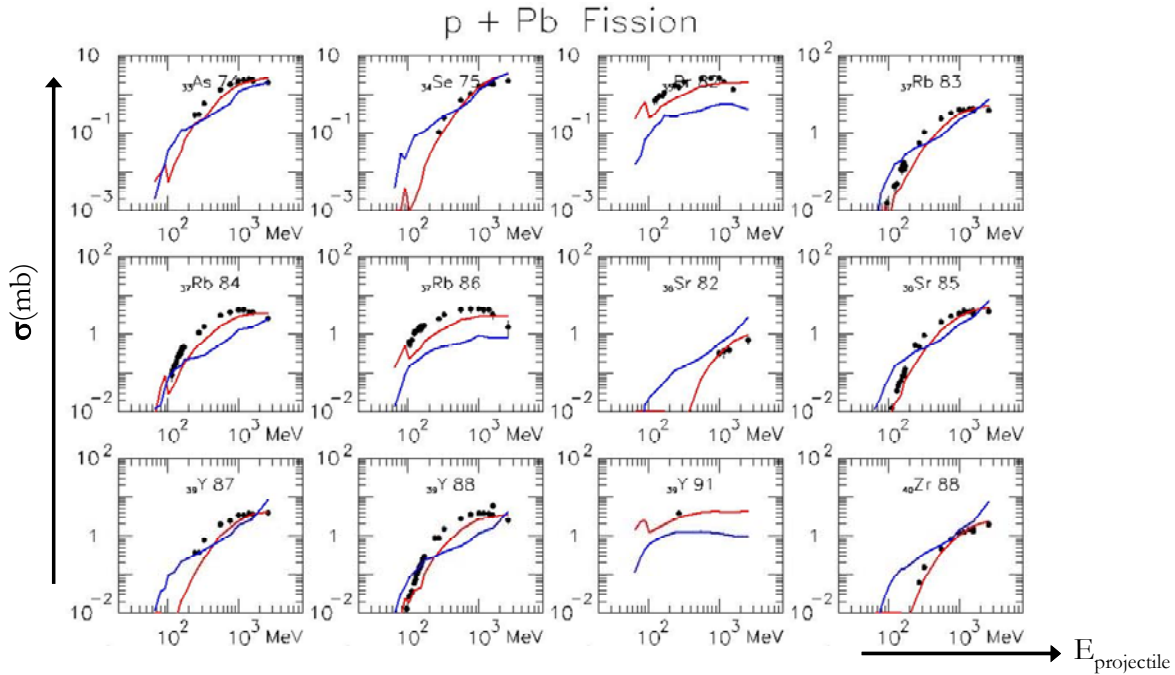

Figure 8: *Excitation functions of the reaction products from p+Pb. Data [9] are in black and models shown are INCL4/Abla in red and Bertini/Dresner/RAL (default option in MCNPX2.5.0) in blue.*

We used also data from [10], where targets were made of uranium (Fig. 9a-e) or thorium (Fig. 10a-f) and with protons from 100 MeV up to 1600 MeV. Here we plot cross sections and calculation/data ratios as well. Only one model is shown, INCL4/Abla. Variations with energy can be quite different according to the isotope considered. In brief, in most of the cases the data/calculation ratios are within a factor 2, however at low energies, say around 100-200 MeV, the agreement might be worse.
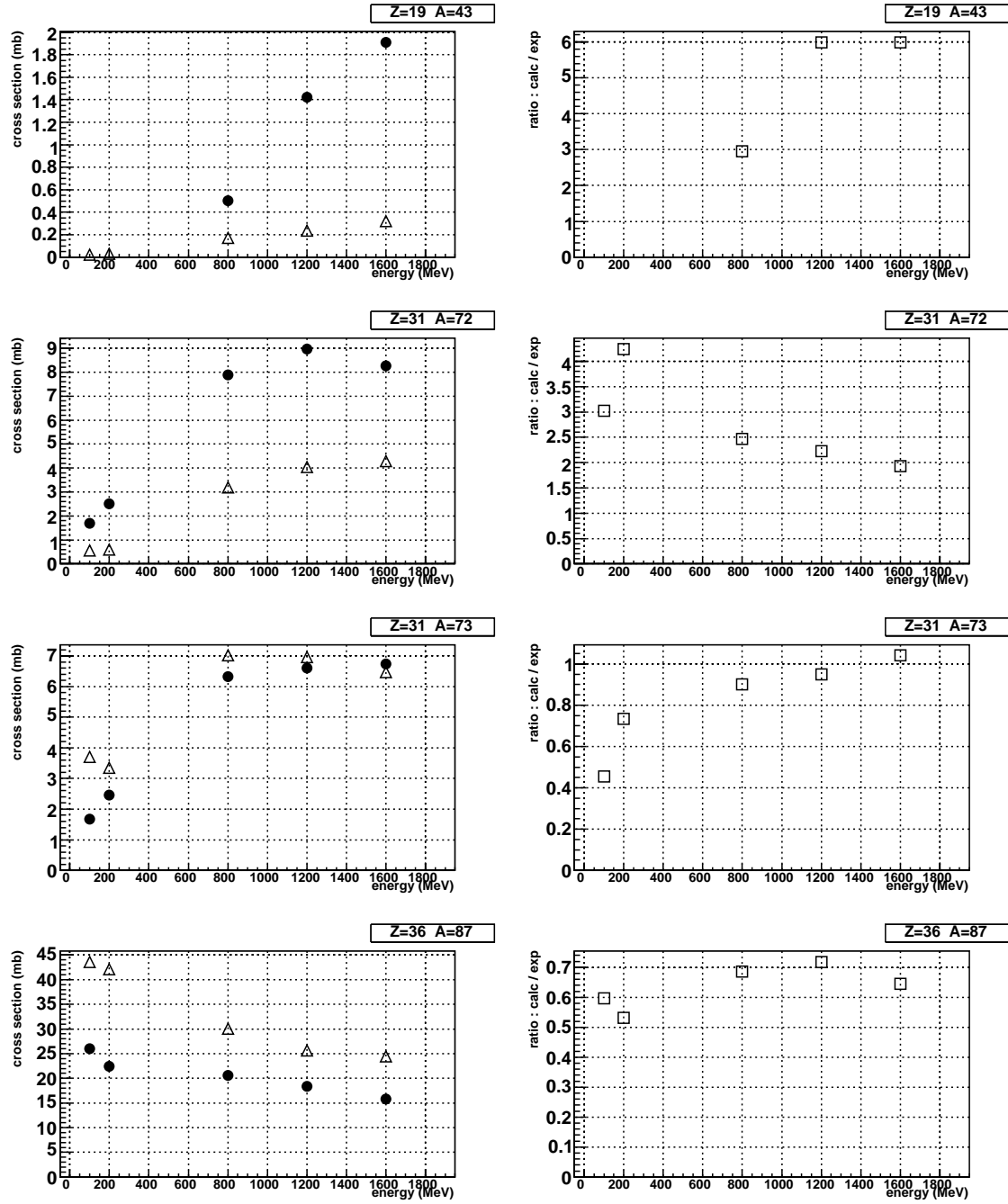
Figure 9a: *Excitation functions of the reaction products from p+U. For each element both absolute cross sections (on the left) and calculation/data ratios (on the right) are plotted. Data [10] are in filled circles and model predictions (INCL4/Abla) are in open triangles.*
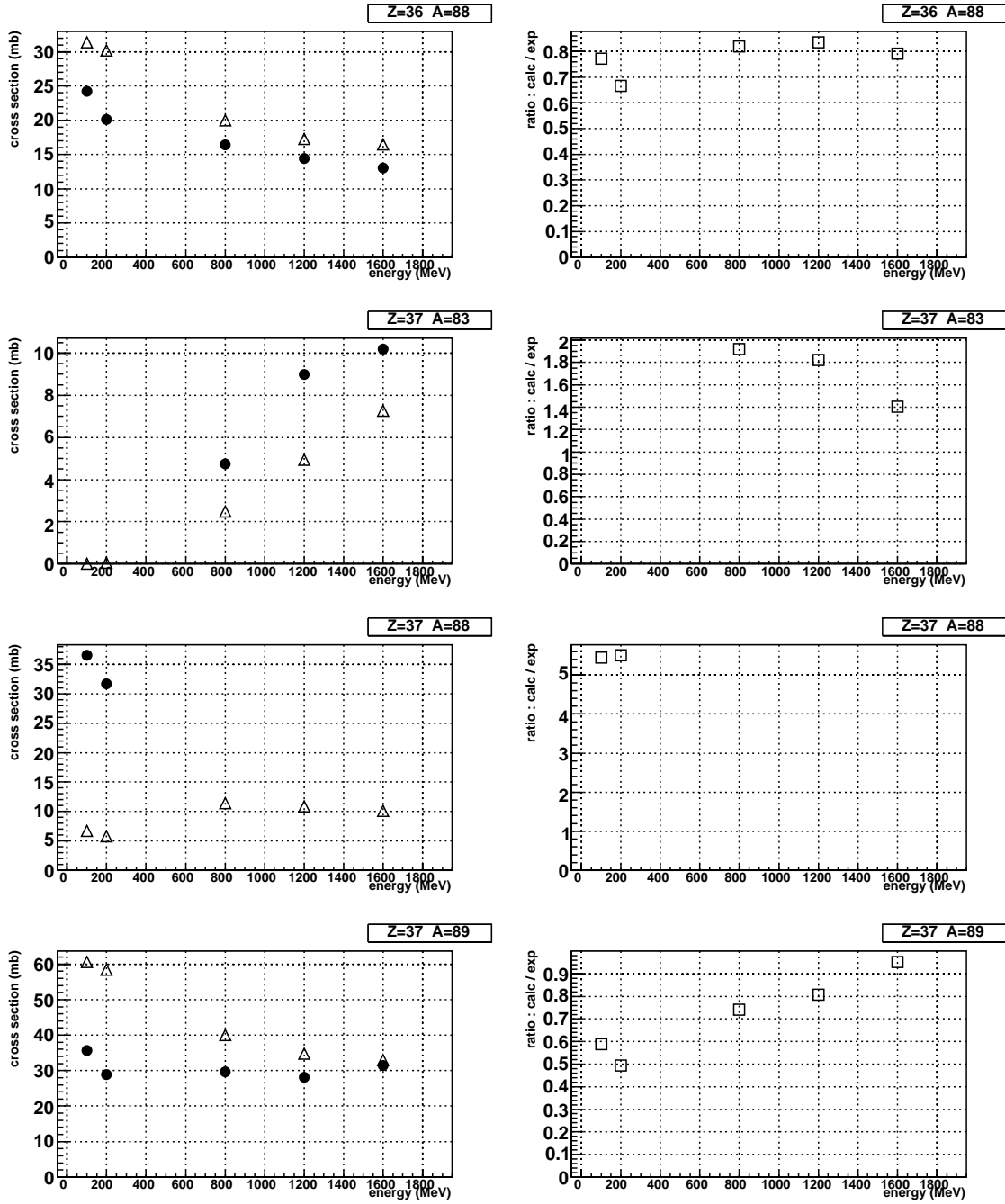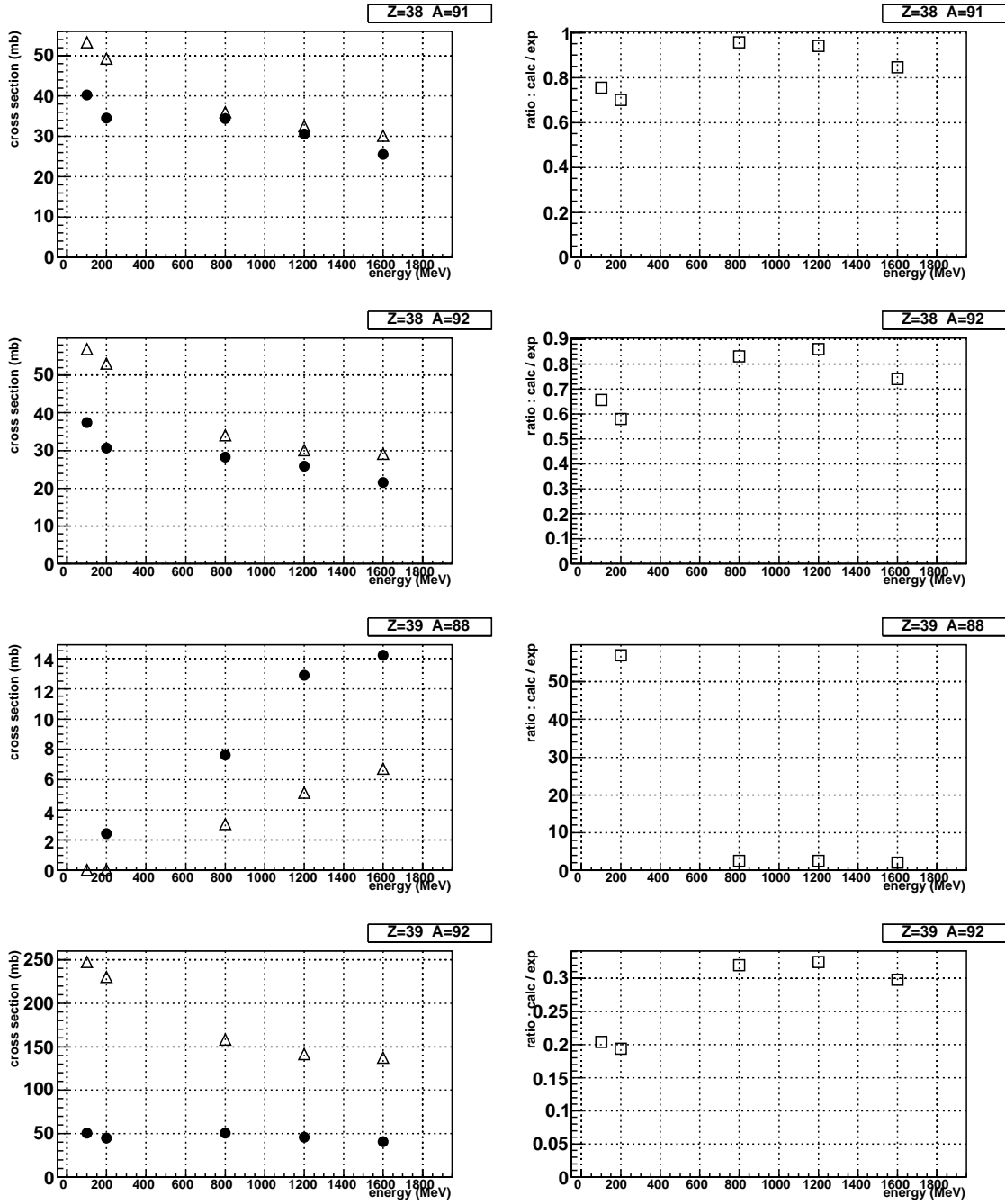
Figure 9b: *Excitation functions of the reaction products from p+U. For each element both absolute cross sections (on the left) and calculation/data ratios (on the right) are plotted. Data [10] are in filled circles and model predictions (INCL4/Abla) are in open triangles.*
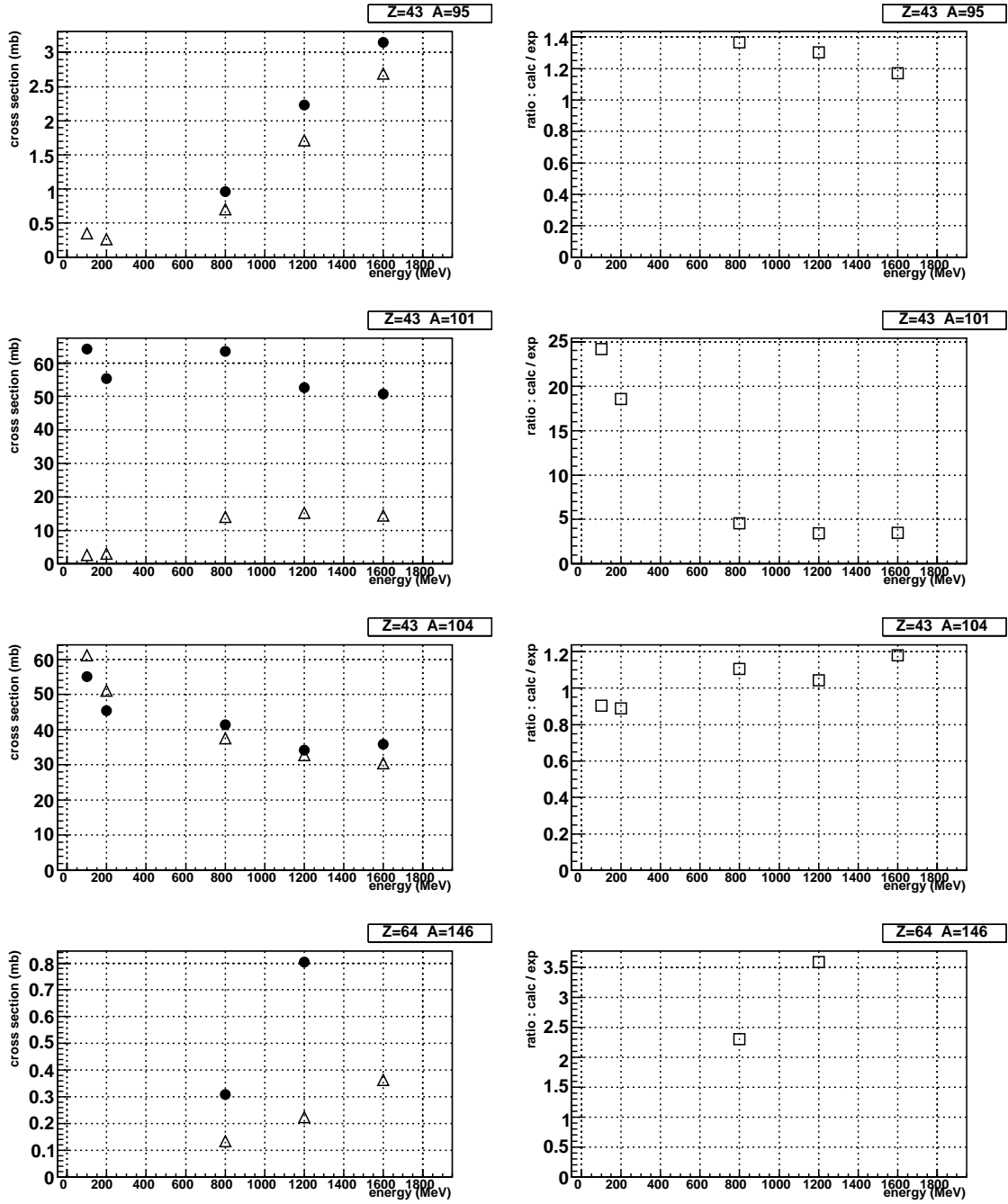
Figure 9c: Excitation functions of the reaction products from p+U. For each element both absolute cross sections (on the left) and calculation/data ratios (on the right) are plotted. Data [10] are in filled circles and model predictions (INCL4/Abla) are in open triangles.

Figure 9d: *Excitation functions of the reaction products from p+U. For each element both absolute cross sections (on the left) and calculation/data ratios (on the right) are plotted. Data [10] are in filled circles and model predictions (INCL4/Abla) are in open triangles.*
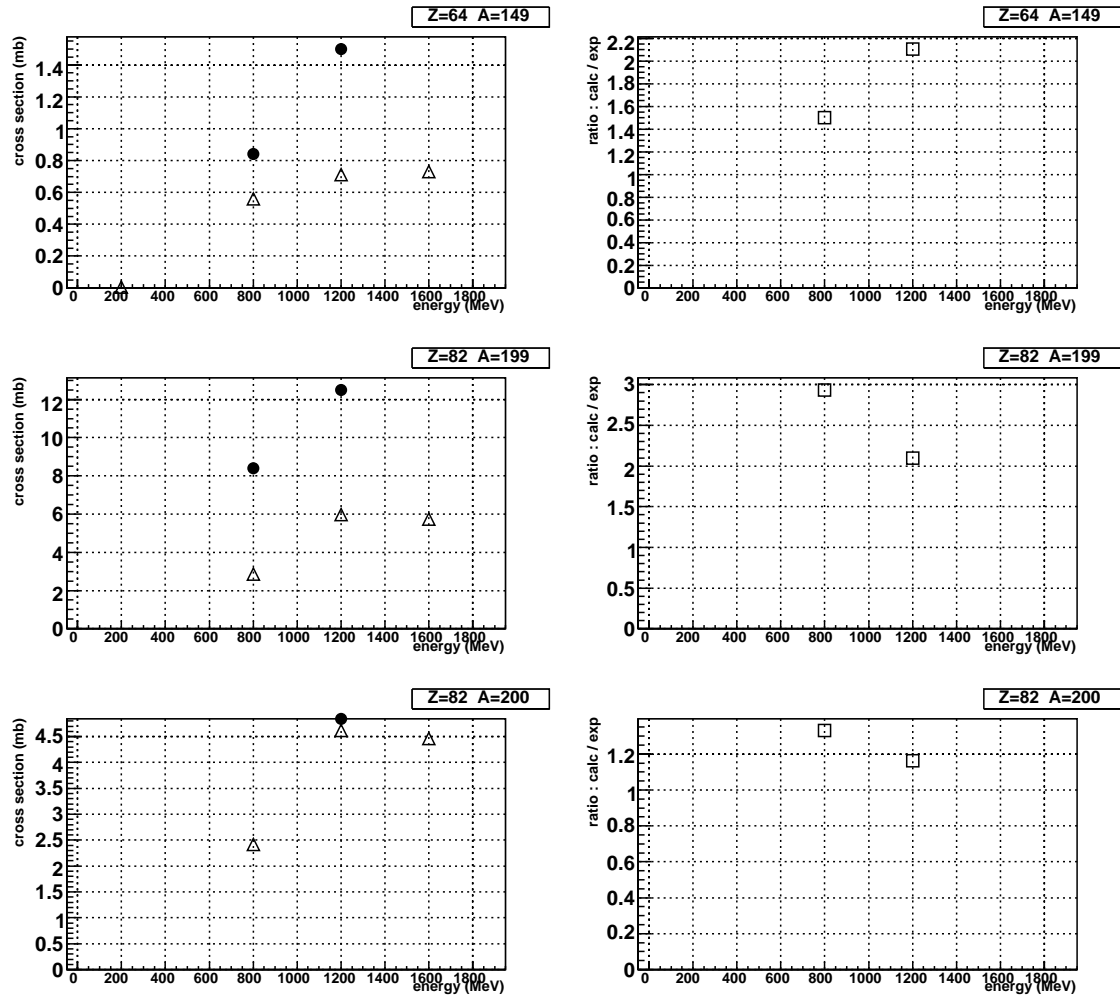
14

Figure 9e: *Excitation functions of the reaction products from p+U. For each element both absolute cross sections (on the left) and calculation/data ratios (on the right) are plotted. Data [10] are in filled circles and model predictions (INCL4/Abla) are in open triangles.*
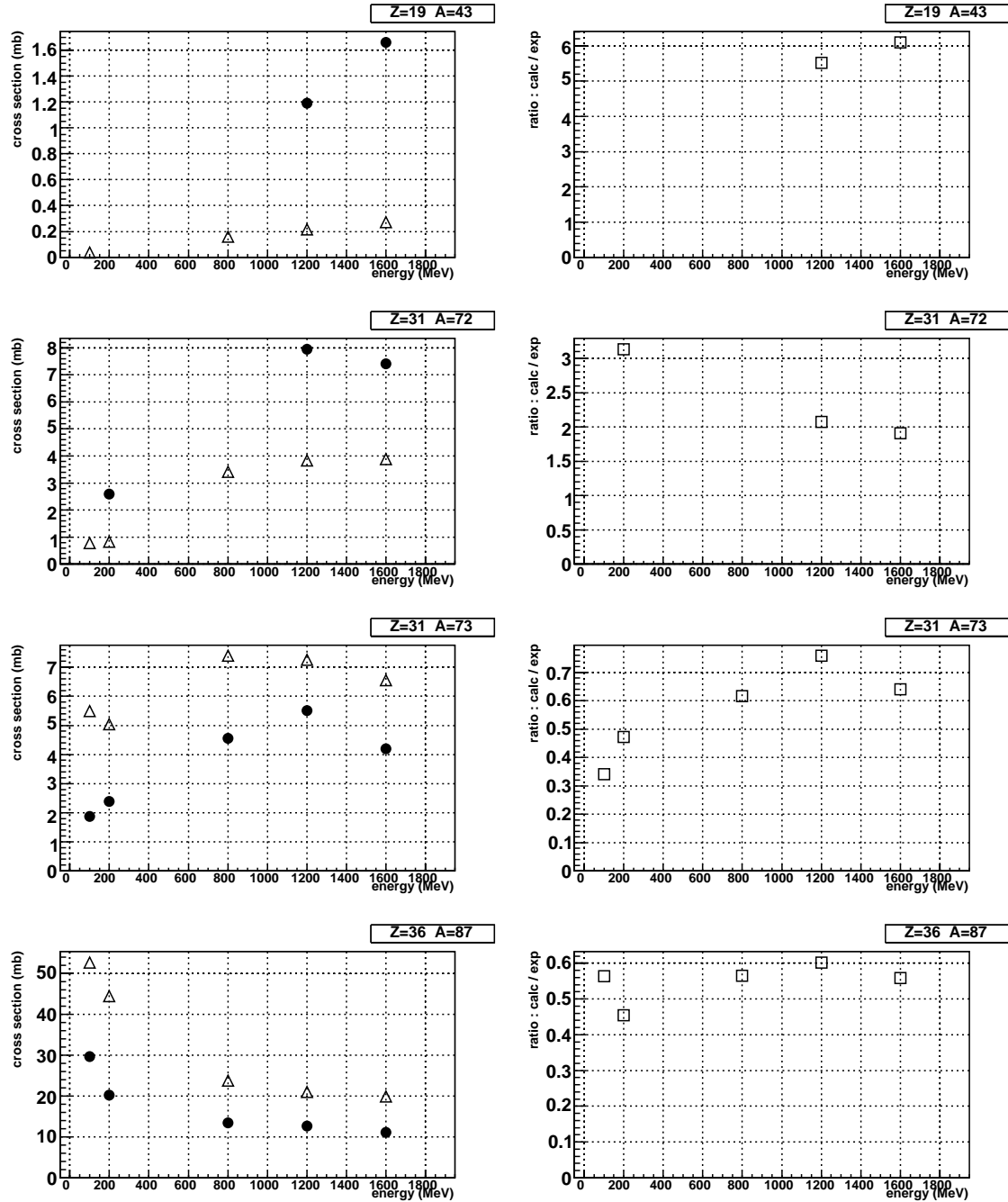
Figure 10a: *Excitation functions of the reaction products from p+Th. For each element both absolute cross sections (on the left) and calculation/data ratios (on the right) are plotted. Data [10] are in filled circles and model predictions (INCL4/Abla) are in open triangles.*
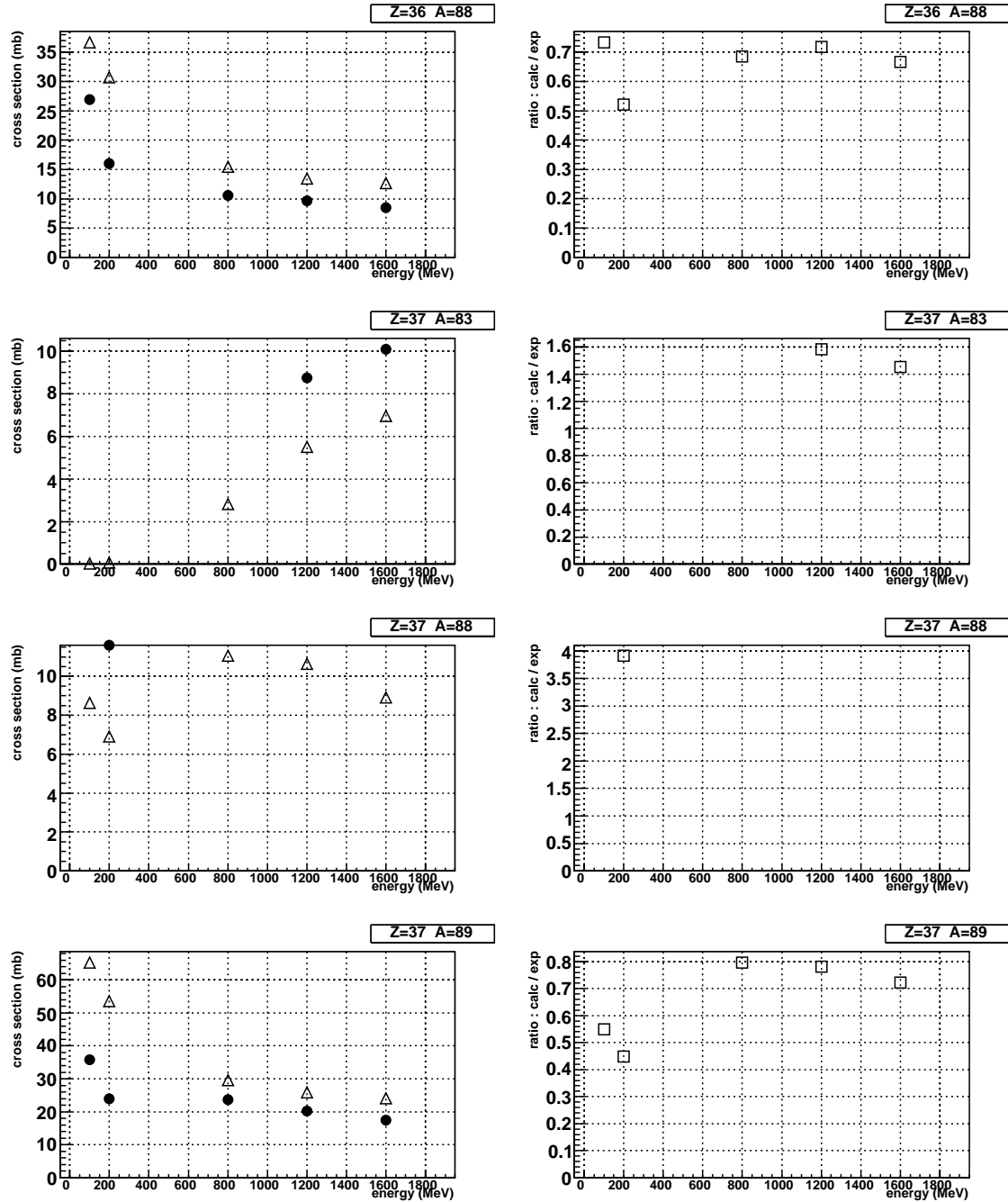
16

Figure 10b: *Excitation functions of the reaction products from p+Th. For each element both absolute cross sections (on the left) and calculation/data ratios (on the right) are plotted. Data [10] are in filled circles and model predictions (INCL4/Abla) are in open triangles.*

Figure 10c: *Excitation functions of the reaction products from p+Th. For each element both absolute cross sections (on the left) and calculation/data ratios (on the right) are plotted. Data [10] are in filled circles and model predictions (INCL4/Abla) are in open triangles.*
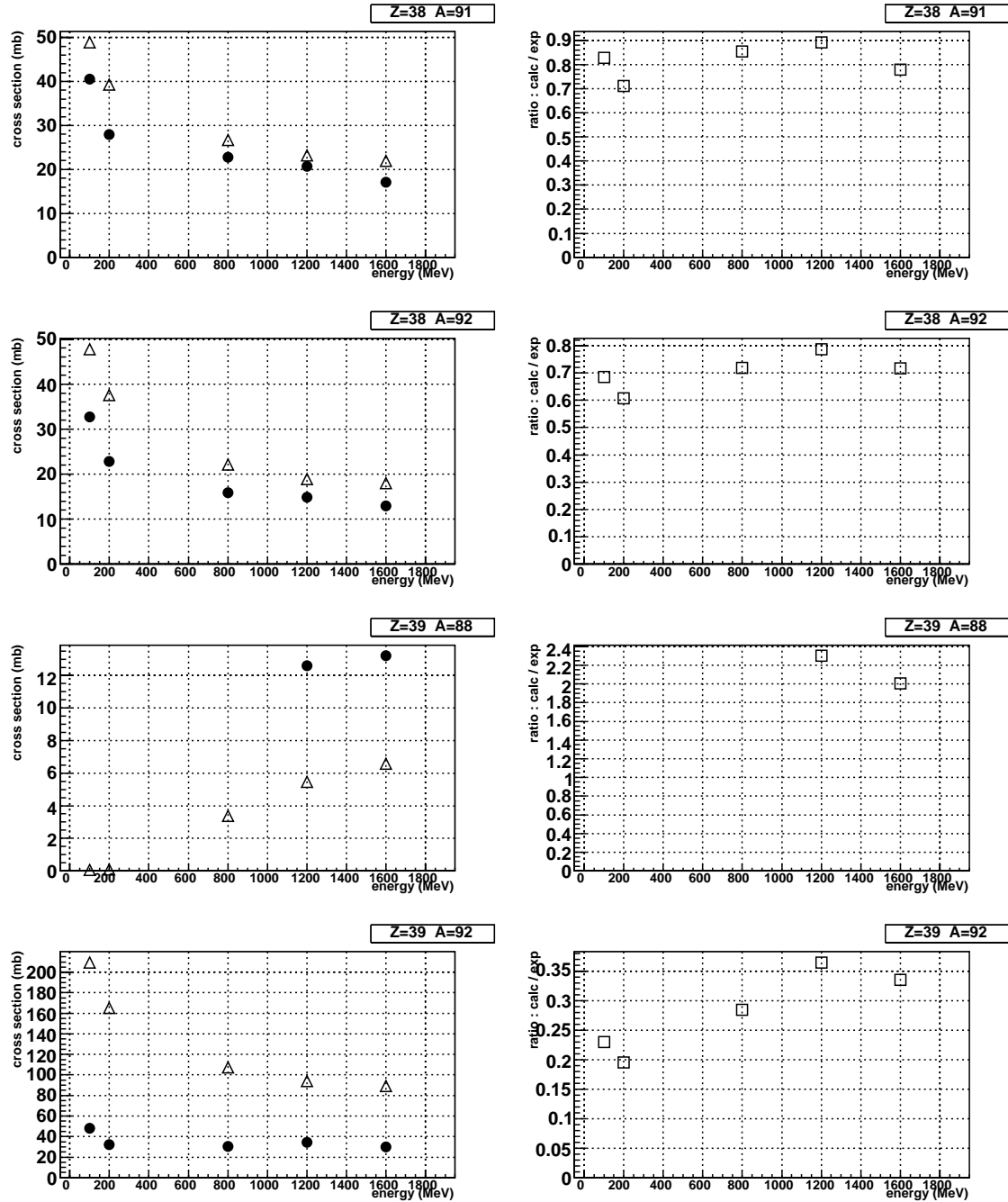
Figure 10d: *Excitation functions of the reaction products from p+Th. For each element both absolute cross sections (on the left) and calculation/data ratios (on the right) are plotted. Data [10] are in filled circles and model predictions (INCL4/Abla) are in open triangles.*
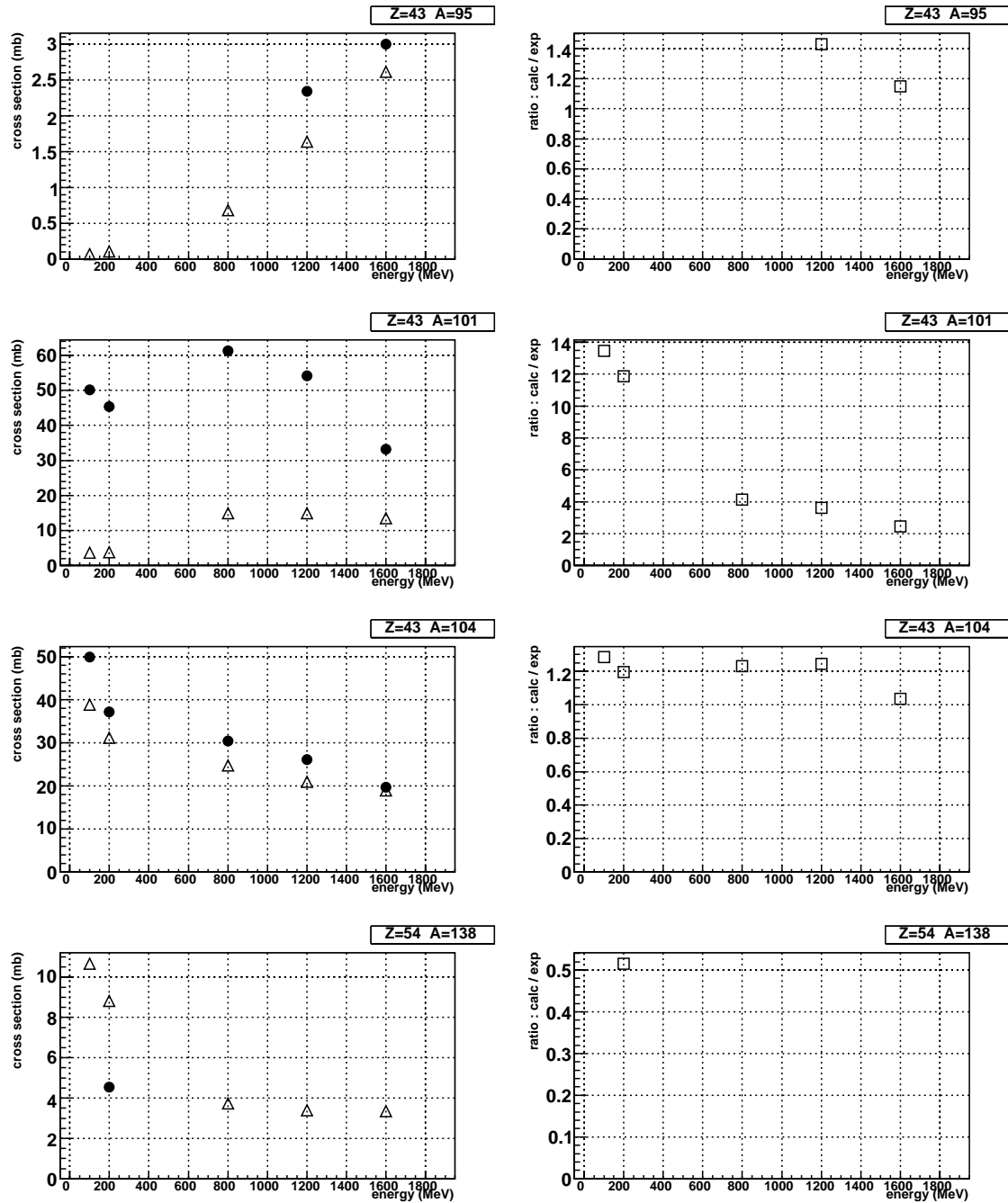
Figure 10e: *Excitation functions of the reaction products from p+Th. For each element both absolute cross sections (on the left) and calculation/data ratios (on the right) are plotted. Data [10] are in filled circles and model predictions (INCL4/Abla) are in open triangles.*

Figure 10f: *Excitation functions of the reaction products from p+Th. For each element both absolute cross sections (on the left) and calculation/data ratios (on the right) are plotted. Data [10] are in filled circles and model predictions (INCL4/Abla) are in open triangles.*
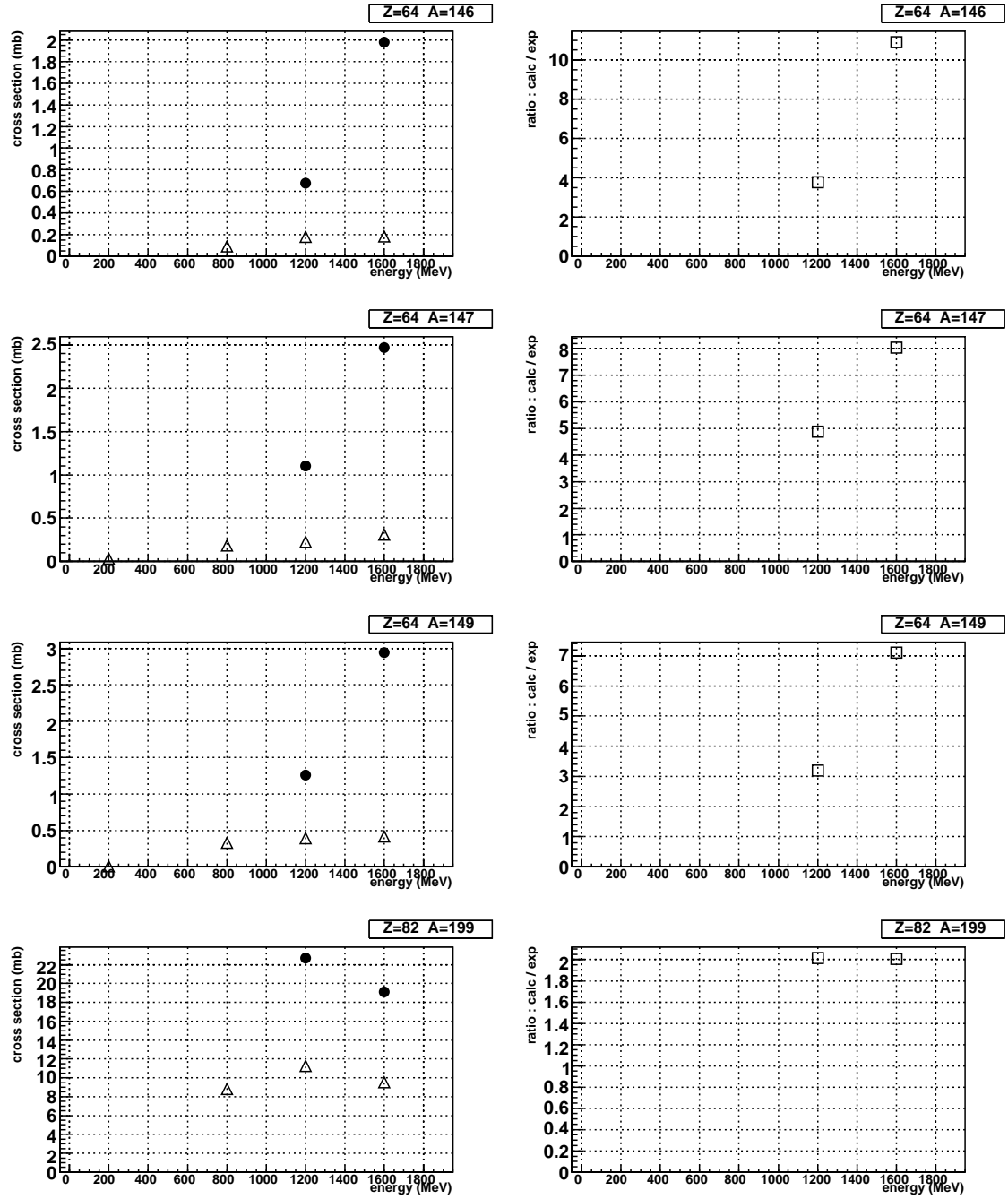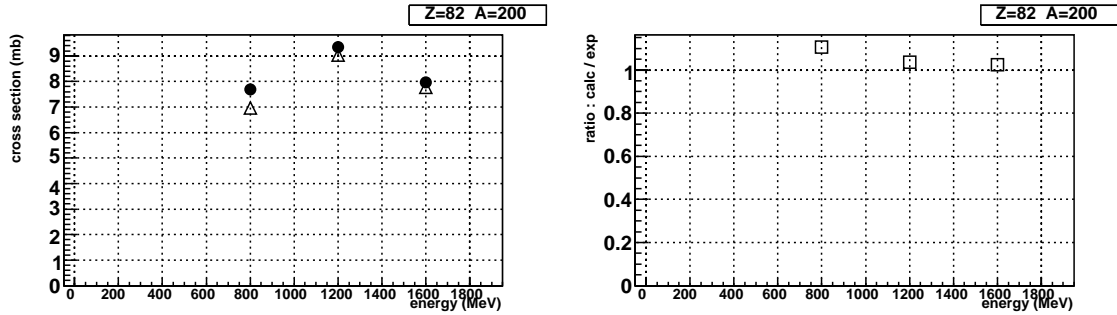
5. Conclusion

Benchmarks on residual nuclei production from proton induced reactions from thin targets were performed (Fe, Au, Pb, Th and U). The MCNPX2.5.0 transport code and the different spallation models available within this code were employed for this purpose. We conclude that presently INCL4/Abla and Isabel/Abla are the best model combinations which we recommend.

A huge number of comparative calculations on mass, isotopic distributions and excitation functions let us conclude that these models fit the data within a factor 2 in most of the cases, except for residues obtained by evaporation far from the target nucleus. We also note that the agreement between model and data are better with ~1GeV protons than with 100-200 MeV protons.

Finally we add that benchmark calculations with thick targets are also needed. Indeed, the residue production in realistic targets is the convolution of the residue production with given projectile energies and the spectrum of the slowing down primary protons and secondary emitted particles during the complex spallation reaction process. Our next report will address this issue.

6. Acknowledgement

References

[1]   More information at http://www.eurisol.org

[2]   "Benchmark calculations on particle production within the EURISOL DS project", B. Rapp et al. , CEA Saclay , Mar. 2006   --- http://eurisol.wp5.free.fr/ (TN-06-04)

[3]   "Validation of FLUKA calculated cross-sections for radioisotope production in proton-on-target collisions at proton energies around 1 GeV", M. Felcini, A. Ferrari, CERN, Jan. 2006   ---   http://eurisol.wp5.free.fr/ (TN-06-01)

[4]   MCNPX User's Manual, Version 2.5.0, April, 2005, LA-CP-05-0369, Denise B. Pelowitz, editor

[5]   More information at http://www.ganil.fr/eurisol/

[6]   More information at http://eurisol-hg-target.web.cern.ch/eurisol-hg-target/baseline%20parameters.htm, http://ab-project-eurisol-ds-direct-target.web.cern.ch/ab-project-eurisol-ds-direct-target

[7]   HINDAS, EC contract fikw-ct-2000-00031, final report (2004)

[8]   M. Bernas *et al.,* Nucl. Phys. A 725 (2003) 213-253 / arXiv nucl-ex/0304003
J. Taieb *et al.*, Nucl. Phys. A 724 (2003) 413-430 / arXiv nucl-ex/0302026
W. Wlazlo *et al.,* Phys. Rev. Lett. 84 (2000) 5736 / arXiv nucl-ex/0002011
T. Enqvist *et al.,* Nucl. Phys. A 686 (2001) 481-524
J. Benlliure *et al.,* Nucl. Phys. A 683 (2001) 513-539
F. Rejmund *et al.,* Nucl. Phys. A 683 (2001) 540-565
C.Villagrasa Canton, Thesis,
« Etude de la production des noyaux résiduels dans la réaction de spallation Fe + p à 5 énergies (300-1500 MeV/A) et application au calcul de dommages sur une fenêtre de système hybride », University of Paris 6, (2003)

[9]   M. Gloris *et al.,* Nucl. Instr. and Meth. A 463 (2001) 593-633

[10]   Yu. E.Titarenko, Experimental and Theoretical Study of the Yields of Residual Product Nuclei Produced in Thin Targets Irradiated by 100-2600 MeV Protons, Final Project Technical report of ISTC 839B-99

[11]   A. Boudard *et al.*, Phys. Rev. C, 66 (2002) 044615)

[12]   Y. Yariv and Z. Fraenkel, Phys. Rev. C, 20 (1979) 2227; Y. Yariv and Z. Fraenkel, Phys. Rev. C, 24 (1981) 488)

[13]   H.W. Bertini, Phys. Rev. 131, (1963) 1801; H.W. Bertini, Phys. Rev. 188, (1969) 1711).

[14]   A. R. Junghans *et al.*, Nucl. Phys. A 629 (1998) 655

[15]   L. W. Dresner, ORNL-TM-196 (1962)

[16]   F. Atchison, "Spallation and Fission in Heavy Metal Nuclei under Medium Energy Proton Bombardment," in Proc. Meeting on Targets for Neutron Beam Spallation Source, Julich, June 11-12, 1979, pp. 17-46, G. S. Bauer, Ed., Jul-Conf-34, Kernforschungsanlage Julich GmbH, Germany (1980)

[17]   J. Barish, T.A. Gabriel, F.S. Alsmiller, R.G. Alsmiller, Jr., 'HETFIS': HIGH-ENERGY NUCLEON - MESON TRANSPORT CODE WITH FISSION. ORNL/TM-7882 (Jul 1981) 26p.

[18]   S. G. Mashnik and A. J. Sierk, "Recent Developments of the Cascade-Exciton Model of Nuclear Reactions," Los Alamos National Laboratory Report LA-UR-01-5390, Los Alamos (2001)

[19]   MCNPX, VERSION 2.6.B**,** June 1, 2006 **-** LA-UR-06-3248 (page 16)

[20]   Radiation Safety Information Computational Center (RSICC) http://www-rsicc.ornl.gov/CODES/CCC/CCC7/CCC-730.html